Proceeding of the IEEE
International Conference on Robotics and Biomimetics
Dali, China, December 2019

A Real-time Needle Tracking Algorithm with First-frame Linear Structure Removing in 2D Ultrasound-guided Prostate Therapy*

Chenliang Tang, Gaosheng Xie, Olatunji Mumini Omisore, Jing Xiong, and Zeyang Xia

***Abstract* - In ultrasound–guided percutaneous interventions, tracking needle tip is always difficult due to the existence of speckle artifact. Moreover, the complexity of prostate tissue increases the difficulties. In this paper, a real-time needle tracking algorithm is presented for localization and tracking of needle's tip in 2D ultrasound images during robotic biopsy and brachytherapy. The proposed method uses image without needle as reference to detect needle insertion in an initial step, and this is followed-up with removal of linear structure in surrounding tissue. Validation for needle localization was performed with 827 sequence frames observed in a prostate phantom. While, the shortest detectable needle length observed is 4.50 mm, shaft and tip localization errors are 1.04 ± 0.35 degree and 0.75 ± 0.6 mm, respectively, and the least tip localization error was 0.06 mm. Meanwhile, a total processing time and single frame average processing time of 33 *secs* and 40 *msec* were achieved, respectively. Thus, our algorithm could track the needle tip in an acceptable tracking accuracy and time useful for robotic prostate therapy.**

Index Terms – ultrasound-guided therapy, needle tracking, linear structure removing.

I. Introduction

In medical surgery, percutaneous interventions require that thin, long, and tubular instruments surgical tools such as needles, imaging probes, and tissue ablation devices are deeply inserted to reach targeted area in the soft tissues. For safe and effective surgical procedures, ultrasound (US) imaging techniques have been augmented into surgical procedures and widely used for real-time visualization during percutaneous interventions [1]. The image-guided technique involves insertion of surgical instruments with trained robotic systems, while feedback information regarding the needle - tissue interactions are utilized for active guidance of the needle along the surgical path. An application of needle tracking is found in brachytherapy interventions used for treatment of tumor in cervical, prostate, and gastrointestinal areas [2].

Despite the numerous works that have been reported, real-time needle visualization remains challenging in scenarios *viz.* 1) when the needle is not completely contained in 2D US imaging plane; and 2) when background tissue contains long, linear objects such as bone, fascia, or tissue boundaries that resemble the needle. Both cases make automatic segmentation of needle to be more challenging. Thus, enhanced image processing methods that increases needle's contrast relative to that of the background structures are required for robust and reliable segmentation of the needle. In addition, continuous identification of needle's tip pose (*i.e.* position and orientation) can help improve targeting accuracy in video sequences. For these purposes, our study is focused towards prostate therapy, but the proposed techniques can be adapted for different kinds of US-guided needle insertion, and applied during both manual and robotic-assisted procedures. The remaining of this paper is presented such that; a review of existing related studies is presented in Section II, while the proposed approach is presented in Section III. The experimental setup used for this study is described in Section IV along with the results obtained. Finally, conclusions drawn and directions for future studies are in Section V.

II. Related work

Several methods have been proposed and described in existing literature to improve needle localization and image-tool tracking during US-guided procedures. These can be roughly divided as hardware-based and software-based methods. The former is add-on component designed as addendum into US imaging system, purposefully for locating needle parts during US-guided procedures. Such methods include using mechanical scoring [3], chemical coating [4] for physical modification of needle's tip, while ultrasonic array adaptive beam steering [5] is also used for enhancing reflection of the needles. Similarly, miniature magnetic sensors, optical tracking sensors are embedded at the tip of a needle, as presented in Kang *et al*. [6]. In addition, needle's tip was reported as having a better visibility in photo-acoustic images, and thus such method can give enhanced needle localization in US images [7].

Despite the pros, locating surgical needle in US images with hardware-based methods increases the cost and complexity of the imaging system. As a result, software-based methods were proposed as dominate alternative. Currently, 2D US is still a standard mostly for clinical interventional surgery.

*Research supported by National Key Project of Research and Development Plan of China Inter-Governmental Cooperative Science and Technology Project (2016YFE0128000), National Science Foundation of China (61773365) and the Fundamental Research Program of Shenzhen (JCYJ20170413162458312).

Chenliang Tang is with Wuhan University of Technology, Wuhan 430070, China, and Shenzhen Institutes of Advanced Technology, Chinese Academy of Sciences, Shenzhen 518055, China.

Gaosheng Xie, Olatunji Mumini Omisore, Jing Xiong and Zeyang Xia are with Shenzhen Institutes of Advanced Technology, Chinese Academy of Sciences, Shenzhen 518055, China.

Corresponding Author: Jing Xiong (Phone: +86-755-86585213; e-mail: jing.xiong@siat.ac.cn).

978-1-7281-6321-5/19//$31.00 ©2019 IEEE

Most software-based methods are built by exploring characteristics of the surgical tools in 2D US images, and processing features like intensity of the needle's tip and shaft. Ding *et al.* [8] developed a performance-optimized Hough transformation technique for real time needle segmentation during biopsy. While the localization accuracy is not guaranteed, no detailed evaluation of needle tip errors was given. Kaya & Bebek [9] used a Gabor-based filter to filter the US image in the pretreatment phase, after the filter is applied, only the information along the insert angle is obtained. However, we note that Gabor-based filters cannot reduce speckle noise at high noise intensities, and execution time of the method is 0.41 ± 0.07 seconds for a single image. Xu *et al.* [10] presented the soft thresholding wavelet technique combining the maximum likelihood estimation sample consensus (MLESAC) algorithm. As a result, the MLESAC-based method showed great robustness in determining needle axis in US sequences. Following, Zhao *et al.* [11] develop a robust needle detection and tracking method using a (region of interest) ROI-Based RANSAC and Kalman Method.. This tracking procedure increases at the same time the calculation speed and the robustness of the technique, which is worthy learning from. However, once the location of the first frame is failed, the tracking would be missing.

Some recent studies have focused on cases where the needle shaft is poorly visible. An attempt with this scenario is the robust intensity invariant method reported in Hacihaliloglu *et al.* [12]. The method uses orientation-tuned Log-Gabor filters with local-phase projections and a best-fit iterative method tagged LMESAC. Results obtained from 150 *ex-vivo* ultrasound scans show an accuracy of 0.41 ± 0.31mm for needle tip localization. However, the method includes using fixed ROI for needle shaft, and requiring images of a certain length needle as reference. On the other side, Kaya *et al.* [13] utilized optical flow to identify the movement of needles in the US images. While this strictly demands that adjacent points in the image always have similar characteristic. Furthermore, Mwikirize *et al.* [14] addressed localization of needles inserted in-plane and out-of-plane, respectively. First, needle tip is enhanced by integrating digital subtraction and a spatial regularization filter, then an object tracking approach based on deep learning is adopted to detect needle tip. The novel method has a tip localization error of 0.72 ± 0.04 mm. However, the model is a multi-object detection framework and it outputted 2D bounding box predictions which greatly decreased the detection accuracy of needle tip.

In real clinical cases, a key challenge is accurate needle segmentation and tracking in US images when the needle's structure is not prominent or its true orientation at entry deviates from the expectation of operators. In these situations, previous needle detection algorithms would locate a false position which lead to unwanted side effects like organ damage or hemorrhage in surgery. Therefore, the main contribution of our study is a real time needle tip tracking strategy with a first-frame linear interference removing link to improve the localization accuracy of the first frame positioning. Meanwhile, we adopt the processing flow in [11] to generate our strategy. It determines the first frame in US sequences by detection of needle's insertion and removes needle-like texture based on background subtraction which is composed of a coarse search strategy and an optimal method for automatic determination of image's resolution. And additionally, needle tip estimation using a set of features around the needle to find the tip location.

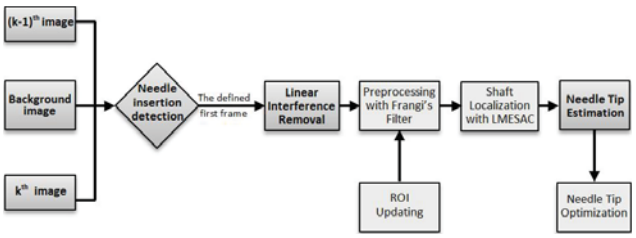

Fig 1. Flowchart of the proposed needle tracking model

III. METHODS

A. Method overview

Linear interference structure in 2D US images may lead to biased or false localization procedure. Besides, it is difficult to detect the needle from the beginning of its insertion.

For this purpose, we propose a needle tracking model, as shown in Fig 1. The first part of the model is focused on initial frame determination during needle insertion. This involves detecting changes of intensity between the first two frames and the background image just before puncturing. Sequel to this, we localize the needle-like structures in the background image with Hough-based method and remove them. The major steps of the proposed model, (shown in Fig. 1, are first-frame linear interference removing, Preprocessing using Frangi's filter, shaft localization with LMESAC, tip estimation, Kalman filter for tip optimization. Details of these are explained below.

B. First-frame linear interference removal

This consists of two major steps, which are given below:

1) Insertion detection

Considering a US frame sequence with temporal continuity, represented by the function *I(x,y,k)* such that *k* denotes the position in the time sequence and *(x,y)* are the corresponding spatial coordinates, the needle is treated as foreground object while the rest of the image is designated as background data. The background image *f(x,y)* without a needle is obtained as the image data before puncturing while the difference image $\Delta I_k(x,y)$ between the background image and *k-th* frame is obtained with the absolute difference given in (1).

$$\Delta I_k(x,y) = | I(x,y,k) - f(x,y) | \quad (1)$$

Due to the localized needle motion and global motion of the tissues during insertion, the classifier function in (2) was defined to distinguish pixels of the needle in $\Delta I_k(x,y)$. For this purpose, intensities of the needle in the image frames were threshold and the parts above the given threshold T is regarded as part of the needle.

$$\Delta I_k(x,y) = | I(x,y,k) - f(x,y) | \quad (2)$$

$$b(x,y) = \begin{cases} 1, if\ \Delta I(x,y) > T \\ 0, otherwise \end{cases} \quad (3)$$

Through (3), we obtain a binary image *b(x,y)* for every current frame, and this is enhanced, as *q(x,y,k)* in (4), with point-wise AND logical operator "^" for proper segmentation of needle in the image. The operation yields only the objects that moved between two successive frames in the US data; thus, an enhanced needle location can be obtained. Following, by counting the non-zero pixel, the first frame can be defined and tracking algorithm start.

$$q(x,y,k) = b_k(x,y) \wedge b_{k-1}(x,y) \quad (4)$$

2) Remove linear interference

Sequel to insertion detection, the linear interference, from tissue contour information and speckle artifacts, usually found in the background image are processed and removed to avoid interference with needle detection during tracking. For this purpose, Hough transform (SHT) is applied to locate the needle-like structure in original image, while the approximate locations of the false detection area can be obtained. Unlike other axle localization methods, SHT is an edge detection algorithm which can be used to detect multiple lines at a time [15]. Thus, we use SHT to locate the expected numbers of interference lines. Essentially, SHT is a mapping relationship from image space to the parameter space. A point on the image plane is converted into a curve in polar coordinates using (5). Further, a line in the image coordinate system is transformed to the intersection point of many curves in the coordinate system shown as Fig. 2. In (5), *r* is the distance from the origin to the line, while ρ is angle of the perpendicular projection from origin to the line measured in degrees clockwise around x-axis. By calculating multiple peaks of the intersection points of parametric space curves, potential interference lines in the input image can be found.

$$r = x \times \cos(\rho) + y \times \sin(\rho) \quad (5)$$

3) Determination of an optimal image resolution

A limitation of SHT is its computational complexity. Thus, we first reduce the image resolution to minimize the computation time required for SHT execution. Here, we utilize the smallest size of a region ($M' \times N'$) containing the non-zero pixels to replace the original size ($M \times N$) of the binary image before puncture *f(x,y)*. M'、N' are defined by (6) and (7).

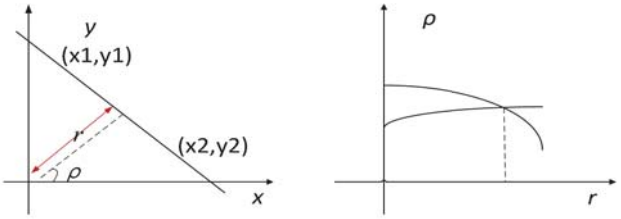

Fig 2. Image Space and Parameter Space

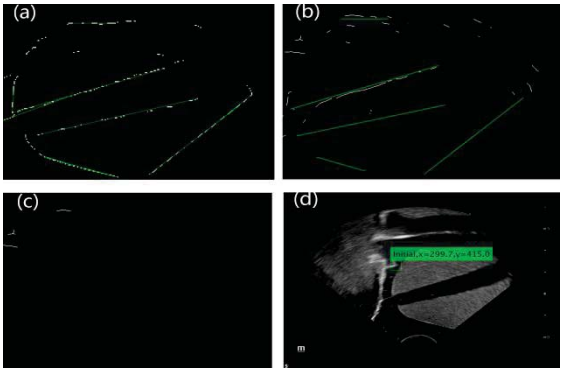

Fig 3. Procedures of image filtering in proposed method: (a) located needle-like interference in *g(x,y)*; (b) linear structure mapping to current binary image *I(x,y)*; (c) needle-like structure removed from

$$\begin{aligned} M' &= x_{\max} - x_{\min} + 1 \\ N' &= y_{\max} - y_{\min} + 1 \end{aligned} \quad (6)$$

where:

$$\begin{aligned} x_{\min} &= \min\{x_i \mid f(x_i, y_j) \neq 0; i \in [1, M]; j \in [1, N]\} \\ x_{\max} &= \max\{x_i \mid f(x_i, y_j) \neq 0; i \in [1, M]; j \in [1, N]\} \\ y_{\min} &= \min\{y_j \mid f(x_i, y_j) \neq 0; i \in [1, M]; j \in [1, N]\} \\ x_{\max} &= \max\{y_j \mid f(x_i, y_j) \neq 0; i \in [1, M]; j \in [1, N]\} \end{aligned} \quad (7)$$

Therefore, optimal image resolution at the coarse stage can be determined by minimizing the computational complexity of the method. Then, its lower resolution image *g(x,y)* is modeled with (8) and (9), where λ_x 、 λ_y are the magnifying factors in the x- and y- axes.

$$g(x,y) = f(\lambda_x x, \lambda_y y) \quad (8)$$

$$\lambda_x = \frac{M}{M'}, \lambda_y = \frac{N}{N'} \quad (9)$$

An instance of applying the SHT method is given in Fig.3. The position and orientation of the needle-like interference structures in *g(x,y)* in Fig.3a can be seen in the coarse stage and the detected lines l_{axis} are mapped to the sequence images *I(x,y,k)* in Fig. 3b. The position and orientation of the detected needle-like interference structures in *g(x,y)* in Fig.3a can be seen and the lines l_{axis} can be mapped to the current image *I(x,y)* in Fig. 3b.

4) Coarse search strategy

Accuracy of localizing needle-like lines are affected by lowering resolution of the US images during needle insertion, and effects of needle-tissue interactions such as prostate deformation. Notwithstanding, position information of the interference lines can be obtained, by defining an area that contains line structure, while the effects of motion artifacts are rather eliminated by approximating the position of the lines. Thus, the needle-like interference lines in the defined regions，P_{areas}, are removed from puncture an image *I(x,y),* as shown in (Fig. 3c), if the condition in (10) is satisfied; where *r* is the expected distances of pixels N to certain estimated lines l_{axis}.

$$P_{areas} = \{N \in P \mid d(N; l_{axis}) \leq r\} \quad (10)$$

C. Preprocessing using Frangi's filter

Frangi's filter [16] is adopted to enhance the needle's contrast while the background's pixels are eliminated. Invariably, this enhances the needle's structure in each frame. The filter was implemented as given in Frangi *et al.* [16].

D. Needle axis localization with MLESAC

MLESAC is a robust estimator and one of the most widely used in the field of line detection. The MLESAC approach fits a model to the best points from a given data set by iterative sampling and fitting to random subsets of the data [17]. In this study, it is adopted to localize needle axis because its operation time is greatly reduced, while the localization accuracy is stabilized by maximizing the likelihood rather than just the number of inliers. Meanwhile, a checking mechanism was added for verifying if the estimated axis is in the same domain at every 5 frames to further improve the localization accuracy. In situations where the estimated axis is not in a similar domain, the located position is replaced with the result of a previous frame.

E. Tip Estimation

For in-plane tracking, once the optimal axis of the needle has been accurately located, the needle tip is estimated. Usually, this is regarded as a point where intensity decreases fastest in the direction of a needle axis. If the US image is noisy or the needle is close to other structures, the needle tip cannot be differentiated as a bounded or an unbounded structure. Therefore, position of the needle tip cannot be recognized unless external position sensors, such as optical tracker, is used. However, in the absence of such external sensors, appropriate needle estimation procedures can be used; and one is proposed in our study. This was done by analyzing the intensity of needle in an estimated axis along with information about the associated box. In addition, the deepest point in needle axis detection is defined as the potential tip P_{tip} while a vector formed along the other side of detected line represents the insertion direction of the needle P_{in}. The proposed method is described with the following stepwise procedures:

Step 1: traverse the straight line and calculate its gradient value in the direction of the estimated needle axis beginning with P_{in}. All pixels above a certain value with a significant decrease in intensity are participant points, and added to P_{tip};

Step 2: calculate the mean of eight-field values g_1 for all points in front of a given step in P_{tip} along needle axis;

Step 3: calculate the mean of eight-field values g_0 for all points with a certain step before P_{tip} along needle axis;

Step 4: calculate the mean of eight-field values g_2 for all points with a certain step before P_{tip} along needle axis, if the participant points do not satisfy (11) for a given threshold (*val*), it will be removed from P_{tip};

$$g_1 - g_2 > val \,\&\&\, g_0 - g_2 > val \quad (11)$$

Step 5: Repeatedly use a sliding window to compute the mean intensity value of the needle along the insertion direction up to each participant points, then a high value of the quantitative needle metric indicates that the needle exist P_{tip} at the window position and a low value suggests that the needle does not exist at the window location. Hence, the needle tip P_{tip} is localized by finding the point along the needle axis that maximizes the value.

F. Kalman filter for tip optimization

The geometrical shape of the needle is very close to a straight line in 2D US images. In real time, there can be fluctuations in the estimated needle tip trajectory because of the estimation noise coming from the algorithm explained above and the dynamics of the control system. Since a Kalman filter [18] is a state estimation algorithm which combines prediction (prior distribution) and measurement update (likelihood), we utilize it for smoothening the estimation noise and optimizing the position of detected needle tip.

IV. Data Acquisition and Experimental Validation

A. Image sequence acquisition

Performance of the proposed needle tracking model was validated with a brachytherapy robot developed for prostate interventions using the experimental setup shown in Fig. 4. Details about specific parts of the robotic setup are given.

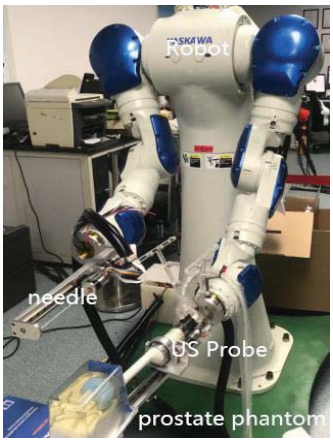

Fig 4. Experimental setup with a dual-arm robot for needle insertion.

1) US Machine

A DC-8 PRO Color Doppler Ultrasound System (Mindray Medical Corporation, Shenzhen, China) is integrated into the robotic setup for acquisition of US images sequences. Before a needle is inserted, the probe is moved to a specified depth for unique acquisition of background image just before puncturing. Sequel to this, the needle is inserted into a prostate phantom while the probe remains stationary. With this process, a data-set of 2D US images are collected. The images have a size of 1050 × 720 pixels with 0.18 mm/pixel in both lateral and axial resolutions; while the frame grabber was set to 35 frames/sec. Thus, it takes circa 30ms to generate one 2D ultrasound image.

2) Brachytherapy Robot

A dual-arm robot (YASKAWA) robotic system, herein tagged as Brachytherapy Robot, was used to insert biopsy needles (PTC Needle 18G, Hakka Co, Ltd) into a prostate

phantom. During the experiment, the brachytherapy needle was mounted as an end-effector of the robot, while a US probe was attached to the other arm to keep the needle's tip always being visible in the 2D US frame plane.

3) US prostate phantom:

This is a 3D prostate phantom with rectal wall, seminal vesicle, perineum and urethra; generally used for validation of procedures that involve prostate scanning with a rectal probe. The US-guided cryosurgery training phantom is designed to minimize needle tracking and provide imaging contrast under CT, MRI, US and elastography.

B. Experimental Result

1) Execution Time

The whole procedure was implemented in MATLAB R2008a on a standard PC workstation which has an Intel® Xeon® with processor speed of 3.10 GHz, RAM 32GB, and Windows 7 (64-bit) operating system. The acquired video sequences contain 827 frames; the detected needle insertion image is, for instance, 245-th image in the scenario given in Fig. 3d, while the detected insertion needle length is 4.5mm in the current image. In the first stage, the execution time of the proposed line-structure removing and tip localization methods for the detected insertion image is 160 msec. In the tracking loop, it takes 40 msec to locate the needle for a single US image. Thereby, we introduced the method that detection is done every two frames and the estimated needle tip is regarded satisfactory for real-time applications. The execution time of the whole method for the insertion image sequences is 33 *sec*.

2) Result

Performance of the proposed tracking method is evaluated based on mean and standard deviation of the needle axis localization error and tip estimation error during the tracking process. The latter is defined as the Euclidean distance between the actual needle tip location and the estimated needle tip location, while the former is a measure of the angle between the estimated shaft and labeled shaft. A ground-truth needle location is created by manually annotating the point belonging to the needle in each frame. This proposed method yields mean localization errors of 1.04 ± 0.35 degree and 0.75 ± 0.6 mm, respectively.

Following the method described in Zhao *et al.* [11], the pretreatment and localization method are only implemented in the first US image to initialize the ROI, while the localization algorithms is run only on the cropped ROI and not the entire image. Similarly, Xu *et al.* [10] in their method tracks the needle by using wavelet soft thresholding method and MLESAC to locate the needle in every frame. It shows that MLESAC is effective and robust in the 2D US image. In this study, we combined the two strategies, and a difference from both studies is that we added a method for an additional step of removing the first-frame linear interference to improve the tracking accuracy.

Comparing the result from our study with method of Zhao *et al.* [10], the latter shows the needle cannot be in the first frame and thus, leading to the tracking failure. Meanwhile, our method defined the first-frame by detecting the needle insertion, removed the linear structure in the defined frame. During the needle insertions, the needle tip was tracked successfully in all the frame sequences using the proposed method. Fig 5 and Fig 6 shows the experimental results for both the axis error and tip error observed when the proposed method and the method in Xu *et al.* [10] were used.

Similarly, the localization results using both methods for tracking needle tip in 2D US images are given in Fig 7. The needle axis and tip localization error values observed with our proposed method varies from 0.10 – 31.17 degree, and 0.06 – 17.73 mm, respectively; while the method in Xu *et al.* [10] has needle axis and tip localization error values varies from 0.15 - 89.97 degree and from 0.19 – 30.43 mm, respectively. That is, the localization error values with the proposed method have lower variation than that of the method in Xu *et al.* [10].

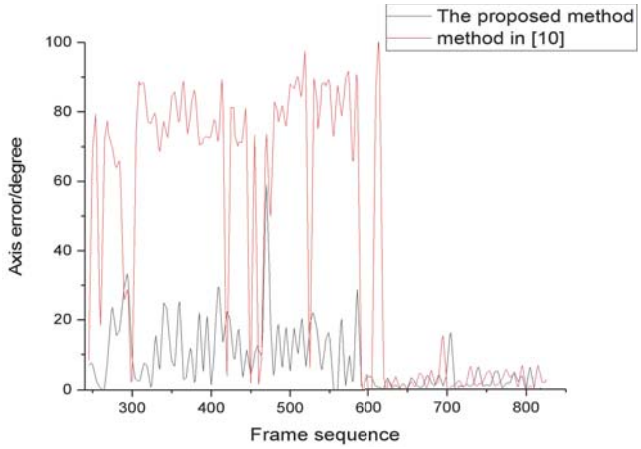

Fig 5. Axis error using the proposed method and the method in [10] for every 5 frames in the sequence images starting with the 245th frame

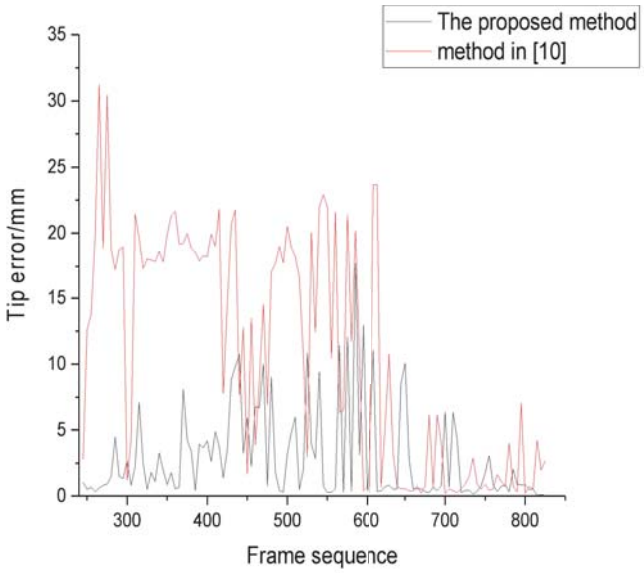

Fig 6. Tip error using the proposed method and the method in [10] for every 5 frames in the sequence images starting with the 245th frame

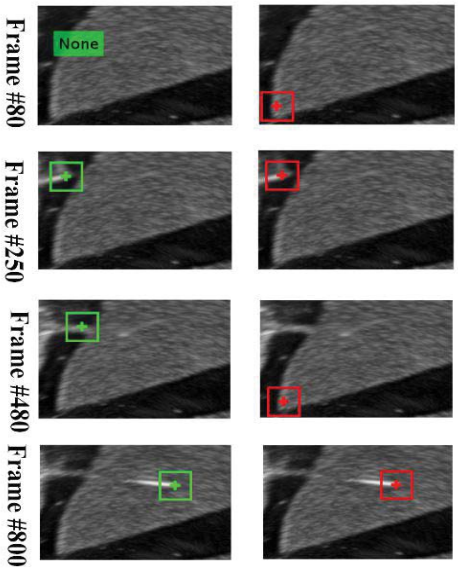

Fig 7. Results using the proposed method (left) and method (right) in [10] tracking needle tip in 2D US images

V. CONCLUSION

Considering that the general methods used for US needle tracking always give a localization result regardless of whether the needle is present or not, we propose a novel needle tracking method enhanced with background subtraction, in this paper. Firstly, we set a needle insertion mechanism to determine when best to start the tracking. Once a ROI is selected, the tracking algorithm is only run on the selected area; thus, ensuring an accurate positioning in the first stage and this is critical to the entire tracking procedure. Further, we utilized information of background image to remove needle-like areas, and combined the improved background image with a linear interference removal algorithm to provide more accurate tip position in the ROI. Results from the experiments performed shows that the proposed method improved the positioning accuracy by removing linear structure in the insertion detected image compared with previous methods in [10][11].

In future work, we will focus on real-time biplane imaging in US-guided treatment. By combining transverse image and sagittal image of needle, the out-plane tracking can be achieved and three-dimensional needle shape can be reconstructed. Furthermore, the accuracy of minimally invasive medical procedures will be further improved.

REFERENCES

[1] Abolhassani N, Patel R, Moallem M. Needle insertion into soft tissue: A survey [J]. Medical engineering & physics, 2007, 29(4): 413-431.

[2] Omisore O., Han S., Ren L., Zhao Z. C., Al-Handarish Y., Igbe T., and Wang L., A teleoperated snake-like robot for minimally invasive radiosurgery of gastrointestinal tumors [C], 18th IEEE International Conference on Autonomous Robot Systems and Competitions, April 25-27, 2018, Torres Vedras, Portugal.

[3] McSweeney I, Murphy B, Wright W M D. Estimation of needle tip location using ultrasound image processing and hypoechoic markers [C]//2014 IEEE International Ultrasonics Symposium. IEEE, 2014: 1876-1879.

[4] Charboneau J W, Reading C C, Welch T J. CT and sonographically guided needle biopsy: current techniques and new innovations [J]. AJR. American journal of roentgenology, 1990, 154(1): 1-10.

[5] Cheung S, Rohling R. Enhancement of needle visibility in ultrasound-guided percutaneous procedures [J]. Ultrasound in medicine & biology, 2004, 30(5): 617-624.

[6] Kang H J, Guo X, Cheng A, et al. Needle visualization using photoacoustic effect [C]//Photons Plus Ultrasound: Imaging and Sensing 2015. International Society for Optics and Photonics, 2015, 9323: 93232Y.

[7] Singh M K A, Parameshwarappa V, Hendriksen E, et al. Photoacoustic-guided focused ultrasound for accurate visualization of brachytherapy seeds with the photoacoustic needle[J]. Journal of biomedical optics, 2016, 21(12): 120501.

[8] Ding M, Fenster A. A real‐time biopsy needle segmentation technique using Hough Transform [J]. Medical physics, 2003, 30(8): 2222-2233.

[9] Kaya M, Bebek O. Gabor filter based localization of needles in ultrasound guided robotic interventions[C]//2014 IEEE International Conference on Imaging Systems and Techniques (IST) Proceedings. IEEE, 2014: 112-117.

[10] Xu F, Gao D, Wang S, et al. MLESAC Based Localization of Needle Insertion Using 2D Ultrasound Images [C]//Journal of Physics: Conference Series. IOP Publishing, 2018, 1004(1): 012037.

[11] Zhao Y, Cachard C, Liebgott H. Automatic needle detection and tracking in 3D ultrasound using an ROI-based RANSAC and Kalman method [J]. Ultrasonic imaging, 2013, 35(4): 283-306.

[12] Hacihaliloglu I, Beigi P, Ng G, et al. Projection-based phase features for localization of a needle tip in 2D curvilinear ultrasound [C], International Conference on Medical Image Computing and Computer-Assisted Intervention. Springer, Cham, 2015: 347-354.

[13] Kaya M, Senel E, Ahmad A, et al. Visual tracking of biopsy needles in 2D ultrasound images [C], 2016 IEEE International Conference on Robotics and Automation (ICRA). IEEE, 2016: 4386-4391.

[14] Mwikirize C, Nosher J L, Hacihaliloglu I. Learning needle tip localization from digital subtraction in 2D ultrasound [J], International journal of computer assisted radiology and surgery, 2019: 1-10.

[15] Mukhopadhyay P, Chaudhuri B B. A survey of Hough Transform [J]. Pattern Recognition, 2015, 48(3): 993-1010.

[16] A. Frangi, W. Niessen, K. Vincken, and M. Viergever, "Multiscale vessel enhancement filtering," in Medical Image Computing and Computer-Assisted Intervention MICCAI98. Springer Berlin Heidelberg, 1998, vol. 1496, pp. 130–137.

[17] Torr P H S, Zisserman A. MLESAC: A new robust estimator with application to estimating image geometry [J], Computer vision and image understanding, 2000, 78(1): 138-156.

[18] Geraldes A A, Rocha T S. A neural network approach for flexible needle tracking in ultrasound images using kalman filter [C] 5th IEEE RAS/EMBS International Conference on Biomedical Robotics and Biomechatronics. IEEE, 2014: 70-75.